Author/s:
Sniderman, JMK;Hellstrom, J;Woodhead, JD;Drysdale, RN;Bajo, P;Archer, M;Hatcher, L

Title:
Vegetation and Climate Change in Southwestern Australia During the Last Glacial Maximum

Date:
2019-02-16

Citation:
Sniderman, J. M. K., Hellstrom, J., Woodhead, J. D., Drysdale, R. N., Bajo, P., Archer, M. & Hatcher, L. (2019). Vegetation and Climate Change in Southwestern Australia During the Last Glacial Maximum. Geophysical Research Letters, 46 (3), pp.1709-1720. https://doi.org/10.1029/2018GL080832.

Persistent Link:
https://hdl.handle.net/11343/285421

Sniderman Kale (Orcid ID: 0000-0002-3963-4049)
Hellstrom John, Charles (Orcid ID: 0000-0001-9427-3525)
Woodhead Jon (Orcid ID: 0000-0002-7614-0136)
Drysdale Russell (Orcid ID: 0000-0001-7867-031X)

Vegetation and Climate Change in Southwestern Australia During the Last Glacial Maximum

J. M. K. Sniderman[1]*, J. Hellstrom[1], J. D. Woodhead[1], R. N. Drysdale[2], P. Bajo[1,2] M. Archer, [3] and L. Hatcher[4]†

[1]School of Earth Sciences, University of Melbourne, Victoria 3010, Australia. [2]School of Geography, University of Melbourne, Victoria 3010, Australia. [3]School of Biological, Earth and Environmental Sciences, University of New South Wales, NSW, Australia. [4]CaveWorks, Margaret River, WA 6285, Australia

Corresponding author: J.M.K. Sniderman (kale.sniderman@unimelb.edu.au)

†Deceased

Key Points:

- U-Th dated speleothem palynology illustrates the timing and duration of the Last Glacial Maximum (LGM) in Western Australia
- Between 28-18 ka, the forested far southwest of Western Australia was essentially a treeless shrubland
- The pattern of LGM climate change is coherent with records from other mid-high latitude Southern Hemisphere regions

Abstract

The nature and duration of the Last Glacial Maximum (LGM) in Australia are poorly understood, with little regional agreement on the timing and direction of LGM climate changes. One reason for this is that Australian Late Pleistocene terrestrial sediments typically are both sparse and inorganic, inhibiting the development of detailed radiocarbon chronologies. To address this problem, we extracted fossil pollen from radiometrically dated stalagmites collected in southwest Western Australia. Our pollen record, supported by 30 U-Th dates, reveals the vegetation response to Late Pleistocene climates between ~34-14 ka, through the body of the LGM. Before ~28 ka, sclerophyll forests were more open than today, but at ~28 ka forest cover was essentially eliminated, and treeless conditions were maintained until progressive reforestation at ~17.5 ka. This ~10 ka-long full glacial episode correlates with other mid-high latitude Southern Hemisphere records, suggesting that LGM environmental changes were closely coordinated across the hemisphere.

Plain Language Summary

This study uses fossil pollen extracted from radiometrically dated stalagmites to document detailed vegetation and climate changes that occurred in the southwest of Western Australia at the peak of the last ice age. Today this region is the only part of southwest Western Australia that supports forests, yet for ca. 10,000 years between ca. 28,000 and 18,000 years ago, eucalypt strongholds collapsed and the dominant vegetation type appears to have been shrublands. The timing and duration of full glacial conditions in southwest Australia are very similar to patterns of glacial environmental change observed in other mid-high latitude regions of the Southern Hemisphere.

1 Introduction

Despite half a century of paleoenvironmental investigation of the LGM – the culmination of the cooling trend of the last glacial cycle (Bowler, 1971; Bowler et al., 1976; Dury, 1967; Galloway, 1965; Turney et al., 2006; Williams et al., 2009) – the climatic expression of this interval in Australia remains poorly understood. Recent reviews of Australian Late Pleistocene climate proxy evidence (Petherick et al., 2013; Reeves et al., 2013) concluded that environmental responses between ca. 30-15 ka are contradictory, with regional variations in the timing, magnitude, and apparent sign of moisture changes. For example, pollen and fluvial/geomorphic indicators of moisture balance provide apparently conflicting impressions of LGM hydroclimate, indicating that widespread treeless landscapes coincided with relatively high water availability (Fitzsimmons et al., 2015). Attempts to explain this contradiction have variously invoked Australia's wide range of climate regimes (Fitzsimmons et al., 2013), pointed to the currently poor understanding of the relationships between rainfall and run-off (Petherick et al., 2013), or emphasized the difficulties of quantifying the physiological impacts of lower temperatures and reduced atmospheric CO_2 on vegetation (Hesse et al., 2004). However, a widely acknowledged (Petherick et al., 2013; Reeves et al., 2013; Turney et al., 2006) lower-order problem in understanding Australian LGM climates simply relates to the fact that many Late Pleistocene records have poorly resolved chronologies (Fig. S1, Table S1), which may in part explain the persistent difficulty correlating paleoclimatic events or episodes, at a continental scale.

In contrast to this uncertain Australian palaeoclimate record, it is increasingly evident from a range of proxies, including $\delta^{18}O$ records from Antarctic ice cores (WAIS Divide Project Members, 2013; Stenni et al., 2010), sediment proxies for sea-surface temperature (Barrows et al., 2007) and dust transport (De Deckker et al., 2012) in the Australasian region, and pollen records in New Zealand (Newnham et al., 2007; Vandergoes et al., 2013) and South America (Heusser and Heusser, 2006), that within the mid-high southern latitudes patterns of change around the LGM were tightly synchronized. These records collectively indicate that the Southern Hemisphere LGM can be characterized by a distinct plunge into minimum glacial temperatures and atmospheric CO_2 (Bereiter et al., 2015) at ca. 28 ka, after which full glacial temperatures were maintained for ca. 10 kyr, until deglacial warming and rising atmospheric CO_2 (Parrenin et al., 2013; Pedro et al., 2012) terminated the LGM at ca. 18 ka. Nevertheless, the impression of spatially and temporally asynchronous Australian environmental changes during the LGM has been so strong that some recent reviews (Reeves et al., 2013) expressed skepticism that events documented in Antarctica might be registered as far away as Australia, suggesting instead that the more coherent regional climatic history evident in the North Atlantic region results from the much greater amplitude of Late Pleistocene climate change there, compared to Australia.

A better understanding of the spatial and temporal patterns of Late Pleistocene climate change in Australia may require new, detailed, and accurately dated records of Australian terrestrial environments that extend through the LGM. However, opportunities to develop high quality terrestrial paleoenvironmental records in Australia are limited because tectonic inactivity, meagre glaciation, and the low productivity of glacial era vegetation together reduced the quantities of fine-grained, organic sediment mobilized and accumulated during the Late Pleistocene. Australian Late Pleistocene terrestrial sediments thus tend to provide poor targets for radiocarbon dating, which has impeded the development of a robust chronological framework of glacial climate changes.

Here, we address this problem by presenting a radiometrically dated stalagmite-derived fossil pollen record of Late Pleistocene vegetation and climate change in the far southwest of Australia (Fig. S2). The Late Pleistocene environmental and climate history of southwestern Western Australia is little known. Previously published evidence of its biota and climate are confined to relatively coarsely dated fossil wood (Burke, 2004; Dortch, 2004) and vertebrate assemblages (Faith et al., 2017) recovered during archaeological cave excavations; and a marine sediment pollen record offshore of the south coast of Western Australia (van der Kaars et al., 2017), which provides a spatially generalized picture of vegetation change throughout the last glacial cycle, but includes no samples within the 30-20 ka window. Aspects of the vegetation and climate history of the southwest have been documented through Holocene lacustrine pollen records (e.g., Dodson and Lu, 2000; Gouramanis et al., 2012; Itzstein-Davey, 2004), but none of these records have extended into the Pleistocene. For this reason, we turn to speleothem palynology (McGarry and Caseldine, 2004; Sniderman et al., 2016), the recovery of fossil pollen from radiometrically dated speleothems (secondary cave carbonates including stalagmites and flowstones).

2 Materials and Methods

2.1 Mammoth Cave

We analyzed two stalagmites from Mammoth Cave (34.06°S, 115.03°E), in the Leeuwin-Naturaliste region, formed within the Tamala Limestone (Brooke et al., 2014; Lipar and Webb, 2014), a Pleistocene aeolianite which extends along the southwestern Western Australian coastal margin (Fig. S2b).

Mammoth Cave is a popular tourist cave ca. 30 m deep, supporting abundant speleothem growth. The cave is a sinuous tunnel ca. 250 m long (Fig. S3), well ventilated by openings at each end, through which a small stream flows In broad terms, the vegetation of the Leeuwin-Naturaliste region is an open forest mosaic dominated by a mixture of three Myrtaceae species, jarrah (*Eucalyptus marginata*) and marri (*Corymbia calophylla*) on drier sites, and karri (*E. diversicolor*) on more moisture-retentive and higher rainfall sites, with understories dominated by sclerophyllous shrubs (Beard, 1981). The vegetation immediately surrounding the cave is a tall karri forest (Fig. S1). Mean annual temperature and precipitation, as recorded at Witchcliffe, 7.5 km northeast of Mammoth Cave, are 16°C and 958 mm per year, respectively, with ca. 87% of precipitation falling in the winter half-year (April-Sept). Precipitation in the southwest is predominantly derived from frontal troughs embedded in the mid-latitude westerlies, which shift equatorward during winter, and poleward during summer (Sturman and Tapper, 2006). The stalagmites were collected in 2010/2011 by Lindsay Hatcher, then Natural Environment and Projects manager at Caveworks.

2.2 U-Th Geochronology

U-Th dating was undertaken at The University of Melbourne following (Hellstrom, 2003) and (Drysdale et al., 2012). Speleothem calcite samples of up to 200 mg were dissolved in concentrated HNO_3, spiked with a mixed ^{236}U-^{233}U-^{229}Th tracer and equilibrated on a hotplate overnight. U and Th were separated from the speleothem matrix and collected together using Eichrom TRU resin, then dried down. Samples were then introduced to a Nu Instruments Plasma MC-ICP mass spectrometer in dilute HNO_3 with trace HF via a Nu Instruments DSN desolvator with teflon nebuliser. All isotope ratios were determined simultaneously with the use of dual SEM ion counters for ^{234}U and ^{230}Th. Stratigraphic constraint was used following (Hellstrom, 2006) to determine that the initial $^{230}Th/^{232}Th$ activity ratio for MC-2 was 0.43 ± 0.043. All samples from both stalagmites had corrected ages calculated using this value and its uncertainty, equation 1 of (Hellstrom, 2006) and the ^{234}U and ^{230}Th half-lives of (Cheng et al., 2013). Age-depth model envelopes were constructed using the Monte-Carlo finite positive growth rate model (Scholz et al., 2012) of

(Drysdale et al., 2012) and (Hendy et al., 2012) with sections between hiatuses treated independently and extrapolated to hiatus depths (Fig. 1).

2.3 Pollen sampling and analysis

The processes governing the transport of pollen onto speleothem surfaces, and its preservation within the growing calcite matrix, are poorly understood compared to the corresponding processes in wetland basins (Festi et al., 2016; McGarry and Caseldine, 2004). Studies of the pollen content of cave percolation waters have yielded highly variable results (McGarry and Caseldine, 2004), but other studies have found that concentrations of wind-pollinated pollen types within speleothems decays rapidly with distance from a cave entrance (Burney and Burney, 1993). The latter suggests that pollen delivery onto speleothem surfaces is primarily by airborne transport and/or via animal vectors. This is supported by a survey of speleothems from caves beneath the Western Australian Nullarbor Plain, in which pollen was observed only within speleothems that also contained other evidence (e.g., siliciclastic dust, quartz, fungal spores, and charcoal) of cave ventilation (Sniderman et al., 2016). Cave sediment pollen spectra typically are representative of the surrounding vegetation, and are similar to spectra from nearby outdoor traps or small lakes, though animal-mediated dispersal may be increasingly important with increasing cave depth (Burney and Burney, 1993). Because Mammoth Cave is well ventilated, it is thus likely that the pollen content of its speleothems is derived largely through aerial transport (McGarry and Caseldine, 2004). If so, interpretation of pollen spectra from Mammoth cave will be comparable to interpretation of more familiar, wetland pollen records. However, because cave pollen transport data are unavailable for Australia, and because the nearest wetland-based Holocene pollen record is from Byenup Lagoon near Lake Muir (Dodson and Lu, 2000), ca. 160 km SE of Mammoth Cave, the palynological representation of the modern vegetation near Mammoth Cave is uncertain. To address this deficiency, we also analyzed pollen from a Late Holocene Mammoth Cave stalagmite, MC-12, to aid interpretation of pollen changes observed in the Late Pleistocene record of stalagmite MC-2.

Guided by a preliminary U-Th age model, a sampling strategy for stalagmite MC-2 (Fig. S4) was devised to enable precise removal of individual calcite fragments for pollen analysis. Reconnaissance sampling for pollen indicated that samples of 5-10 g would contain useful quantities of pollen. After embedding in resin to bolster the structural integrity of the stalagmite, a slab ~1 cm thick was produced with a standard rock saw. Stratigraphically contiguous slices, nominally ~0.5 cm wide, were cut from this slab, parallel to the main growth axis of the stalagmite, with a thin-bladed miniature rock saw. In this way, it was possible to trace the extent of individual growth layers in three dimensions. We followed a similar approach for stalagmite MC-12 (Fig. S4) where, guided by a U-Th age model, we collected four contiguous samples each representing ca. 500 yr, within the 1.0 to 3.5 ka interval. Subsequent physical and chemical processing of samples from MC-2 and MC-12 were carried out within a high efficiency particulate air-filtered (HEPA) exhausting clean air cabinet in an International Organization for Standardization (ISO) Class 7 clean room.

Fossil pollen typically is present in speleothems in low concentrations (McGarry and Caseldine, 2004), so we used pollen-processing techniques designed to both minimize contamination by modern pollen and to maximize recovery. Previous analyses (Sniderman et al., 2016) of both speleothems containing extremely low concentrations of fossil pollen and 'blank' limestones indicated that rates of contamination with modern pollen were negligible in our clean room facility. Samples were etched in 1 M HCl for 10 minutes to remove the outer ~50-100 μm of calcite, before washing repeatedly in distilled water. Samples were then dissolved in 12 M HCl. The $CaCl_2$-rich solute was diluted approximately four-fold with distilled water before centrifugation at 3600 ppm for 3 minutes, and discarding the solute. The HCl-resistant residues were processed using conventional palynological protocols (K. D. Bennett and Willis, 2001) including concentrated cold HF, 10% KOH, and acetolysis (a 9:1 mixture of acetic anhydride and concentrated sulfuric acid, at 90°C), with modifications for varying organic matter content of individual samples. Residues were dehydrated in ethanol then suspended in glycerol on permanent glass slides.

Where possible, >100 pollen grains were counted from each sample. To achieve this sum, in some cases it was necessary to return to the MC-2 stalagmite slab to recover additional aliquots by tracing the stratigraphy laterally. We estimate that depth sampling errors introduced through this process amount to ±1 mm, representing up to ±60 yr uncertainty. Total mass processed per sample ranged from 2.7 to 38.9 g, with a median of 14.6 g. For the majority of samples, the entire acid-resistant residue was mounted on glass slides and counted under the microscope. Pollen was counted and photographed under compound light microscopy at 640× and 1,600× magnification on a Zeiss Axiolab A1 with N-Achroplan objectives. All identified pollen types were included in pollen sums, with the exceptions of Urticaceae, abundant in some samples (not shown), and, in MC-12, of a small, robust Chenopodiaceae type. We suspect the source plants of these two pollen types grew within the cave entrance and/or doline, and may therefore behave palynologically in a manner analogous to aquatic taxa, which conventionally are excluded from terrestrial pollen sums of lake-derived records. Pollen identifications were made by comparison with the pollen reference collections held by the first author, and with published pollen atlases including the online Australasian Pollen and Spore Atlas (apsa.anu.edu.au). Following square root transformation, pollen data were divided into stratigraphic zones in psimpoll 4.25 (K.D. Bennett, 2005), using optimal splitting by information content. Variance in the pollen data was reduced using principal components analysis, following square root transformation.

3 Results

3.1 U-Th Age models

The U-Th age model of stalagmite MC-2 (Fig. 1) is based on 30 U-Th ages (Table S2), excluding two which, following additional detailed sampling, were rejected as outliers. The stalagmite grew between ca. 37.6 ka and 14.4 ka, with four hiatuses in stalagmite growth interpreted from petrographic observation (Fig. S4), combined with U-Th age-depth distributions. The age model for stalagmite MC-12 (Fig. 1) is based on six U-Th ages. Uninterrupted growth is inferred between ca. 3 ka and 1 ka.

3.2 The Mammoth Cave pollen record

The pollen data are plotted as a percentage diagram (Fig. 2) with the 24 pollen samples represented as bars of varying thickness proportional to their varying duration (ranging between 0.08–1.96 ka), as estimated by the age model (Fig. 1). Gaps in the record, at ca. 33.0–32.0 ka, 30.0–28.5 ka and 26.5–24.0 ka, represent hiatuses in the growth of the stalagmite and samples from which meaningful pollen sums could not be recovered. Pollen sums ranged from 49 to 324, with a median of 203 grains. The composite record of MC-2 and MC-12 is divided into four statistically significant local pollen zones, denoted M-1 through M-3 (in stalagmite MC-2), and M-4 (in stalagmite MC-12).

The late Holocene pollen record (zone M-4) is dominated (35-50% of the pollen sum) by eucalypts (*sensu* Ladiges et al., 1995), encompassing both *Eucalyptus* and *Corymbia*). Accessory pollen types include both wind- and animal-pollinated forest understorey taxa such as Poaceae, Restonaceae, Asteraceae, *Banksia* (Proteaceae) *Opercularia* (Rubiaceae), *Bossiaea* (Fabaceae), Asparagales, and *Tetratheca*/*Tremandra* (Elaeocarpaceae). This combination of wind- and animal-pollinated taxa, with source plants varying from canopy trees to small herbs, suggests that Mammoth Cave speleothem pollen assemblages are not strongly biased against wind-pollinated taxa, as has been observed in some studies of pollen deposition within caves (Burney and Burney, 1993). Perhaps because its two entrances ensure that the cave is well ventilated, the MC-12 record thus appears to represent late Holocene vegetation of southwest Australia in a manner comparable to lake- and wetland-derived pollen records from the region (e.g. Dodson and Lu, 2000; Newsome and Pickett, 1993).

Prior to ca. 29 ka (zone M-1), relatively high eucalypt values indicate substantial tree cover in the far southwest of Western Australia. However, average eucalypt values in this zone (28%) are substantially lower than their average during the late Holocene (zone M-4), of 43%. Conversely, *Banksia*, represented in the modern regional vegetation by several species of forest understory trees or shrubland dominants, is registered in the late Holocene by an average of only 1.7% of the pollen sum, yet in zone M-1 average *Banksia* values are 19%. This difference, along with higher pollen percentage values of other sclerophyllous shrub taxa, including Leptospermeae (Myrtaceae), undifferentiated Myrtaceae (i.e., genus undefined) and *Amperea* (Euphorbiaceae), implies a greater importance of sclerophyll shrubland/heathland in this region during zone M-1, in the late part of Marine Oxygen Isotope Stage 3 (MIS 3)(Railsback et al., 2015), compared to today (Fig. 3). The absence in zone M-1 of most of the understorey taxa that characterize the late Holocene record reinforces the impression of major changes in the floristic composition of the local vegetation between MIS 3 and the late Holocene. These changes are emphasized by the separation of MC-2 and MC-12 samples in ordination space (Fig. S5).

Between c. 30 ka and 27 ka, steeply declining eucalypt values, from 30% to <5% (Figs 2, 3a) indicate wholesale landscape deforestation, which persists until ca. 17.5 ka. During this deforested interval (zone M-2), *Banksia* twice undergoes brief oscillations (at 28-27 ka and 24-22.5 ka) from very low to moderate values (Figs. 2, 3b). *Banksia*-dominated shrublands and woodlands are well represented in pollen-trapping studies (Pickett, 1997), implying that *Banksia* was a structurally dominant component of the local vegetation at this time. Very open, shrubland habitats are further indicated by high values for woody Casuarinaceae and *Pimelea* (Thymelaeaceae), and the monocots Restionaceae and Poaceae.

After ca. 22.5 ka, *Eucalyptus* values remain very close to zero, while *Pimelea* and Restionaceae values decline, and the mainly wind-pollinated shrub and herb taxa Poaceae, Asteraceae, Cyperaceae, Chenopodiaceae achieve higher values. This floristic change is most simply interpreted as a transition to effectively drier conditions within persistently very open vegetation. However, the persistence of *Banksia* and Myrtaceae undif., and of herbs such as *Opercularia*, *Amperea*, and Restionaceae, that today are largely confined to the relatively moist corner of southwest Western Australia, indicate that even during the latter half of zone M-2 effective precipitation was never extremely low. After ca. 17.5 ka, in zone M-3, eucalypts increase steadily to values comparable to those seen in the late Holocene. *Banksia* also increases slightly, but most taxa that dominated during zone M-2 abruptly decline to low values.

4 Discussion and Conclusions

Mammoth Cave is located within the wettest, most heavily forested portion of the ca. 300 km^2 Southwest Australian Floristic Region (Hopper and Gioia, 2004), at an ecotone between widespread open jarrah forests and the most biologically productive forests in southwest Australia, tall open karri forests (Christensen, 1992)(Fig. S2). However, the Mammoth Cave pollen record indicates that during late MIS 3, regional vegetation was substantially more open than today, as indicated by much higher values for *Banksia* than are observed during the Holocene. With the descent into full glacial temperatures at ca. 28 ka, eucalypt-dominated forest cover appears to have been largely eliminated, replaced by shrubland and herbaceous vegetation. This largely treeless vegetation is recorded at the site for the next ca. 10 kyr, until eucalypt-driven reforestation commenced at ca. 17.5 ka. Glacial treelessness in southern Australia, as in many other regions, has been widely interpreted as indicating climates more arid than today (Hope, 1994; Kershaw et al., 1991). However, it is increasingly clear that, by reducing plant water use efficiency, low glacial atmospheric CO_2 may have shifted competition between trees and short-statured vegetation (herbs and shrubs) towards the latter (Prentice et al., 2017). At the same time, potential evapotranspiration was reduced under low glacial temperatures, contributing to greater retention of moisture in landscapes (Scheff et al., 2017). Thus, on one hand, the treeless LGM at Mammoth Cave was very likely a response to substantially colder climates than today, perhaps driven by meteorological conditions such as strong, cold outbreaks of polar air (McGlone, 1988). On the other hand, since low atmospheric CO_2 should have altered competitive outcomes between *Eucalyptus* and shrublands, it remains unclear to what extent deforestation at Mammoth Cave was driven by reduction in effective precipitation (precipitation minus evaporation) (Hesse et al., 2018), since initial deforestation between 28-26 ka coincided with high Restionaceae values (indicative of relatively moist soils) and very low Chenopodiaceae values (indicative of a regional absence of arid-adapted shrublands).

The broader importance of this pattern (Fig 3a-c) is shown by comparison with climate records from Antarctica and from other mid-latitude Southern Hemisphere regions. The Antarctic ice core δ^{18}O records from the West Antarctic Ice Sheet (WAIS Divide Project Members et al., 2015) (WDC, Fig 3i) and Dronning Maud Land (Bazin et al., 2013)(EDML, Fig. 3j) indicate that Antarctica cooled abruptly at c. 27.5 ka, reaching full glacial temperature minima by 27-26 ka, and that these low temperatures were maintained until ca. 21 ka at EDML, and until ca. 18.5 ka at WDC. This ca. 10 kyr-long interval of minimum glacial temperatures is interrupted only by a brief (ca. 1 kyr-long) warm episode centered on ca. 23.5 ka, Antarctic Isotope Minimum 2 (AIM 2, Fig 3j). Deglaciation soon after 18 ka is clearly marked in the Antarctic records, by both rising ice core δ^{18}O and atmospheric CO_2 (Fig. 3k).

Several mid-latitude Southern Hemisphere records confirm the hemispheric scale of this ca. 10 kyr-long, “extended” LGM (Newnham et al., 2007) or “Last Glacial Coldest Period” (Alloway et al., 2007) pattern. For example, pollen records from the South Island, New Zealand (Fig. 3e)(Vandergoes et al., 2013) indicate a deforested landscape between ca. 28–18 ka, interrupted by a brief expansion of shrubs which may correspond to the AIM 2 event in the Antarctic records. Also on the South Island, the Nettlebed speleothem δ^{13}C record (Hellstrom et al., 1998) from Mt Arthur (Fig. 3d) indicates full glacial conditions, mainly reflecting reduction in plant biomass, from ca. 28-27 until ca. 16 ka, coherent with the timing of deforestation and reforestation in the South Island pollen records. The timing of the transition into full glacial vegetation in South America may be similar; at Tagua Tagua, in central Chile (Valero-Garcés et al., 2005), the conifer *Prumnopitys andina* dominates during the LGCP (Fig. 3g), while at Taiquemó (Heusser and Heusser, 2006), in southern Chile (Fig. 3f), Poaceae increases to full glacial values by ca. 30 ka, earlier than this transition in the Australian or New Zealand records. The latter may be consistent with evidence from Patagonia and New Zealand for expansion of mountain glaciers between 38-30 ka, which may reflect enhanced moisture delivery during late MIS 3 (Shulmeister et al., 2018), prior to the initiation of minimum glacial temperatures at ca. 28 ka. Within southeastern Australia, temperature-sensitive climate proxies from marine sediments offshore of the Murray River (De Deckker et al., 2012) indicate cool and dusty glacial conditions between ca. 28-18 ka, interrupted by a warmer, less dusty interval at ca. 23.5 ka (Fig. 3h). Millennial-scale oscillations of *Banksia* values (Fig. 3b), between ca. 31.5-29.5 ka, 28-26.5 ka, and 24-22.5 ka, appear to be closely coupled to short-lived speleothem growth hiatuses and/or intervals lacking pollen. Tentatively, these brief cycles of growth cessation followed by increasing *Banksia* values may represent expressions of the millennial-scale warming events observed in Antarctic ice cores (AIM events, (Stenni et al., 2010). The clearest example is the *Banksia* peak centered at 23 ka. Allowing for age model uncertainties, this peak appears to match comparable events in the ice core δ^{18}O (Fig 3i,j), in the Murray Canyons Ti record (Fig. 3h), and in the New Zealand Galway Tarn pollen record (Fig. 3e), implying that these brief warming events may have been transmitted rapidly across southern latitudes.

The timing and duration of deforestation in the Mammoth Cave pollen record thus seems to be a regional expression of a coherent, hemisphere-wide LGM pattern. How far north this characteristic Southern Hemisphere glacial maximum pattern extended is uncertain. A sediment record from Tortoise Lagoon, in southeast Queensland at ca. 27.5°S, exhibits double peaks in clastic sediment flux (Petherick et al., 2017), perhaps correlating to the palynologically distinctive early and late portions of zone M-2 at Mammoth Cave. This implies that the ca. 28-18 ka LGM pattern, and perhaps the AIM 2 event, can be detected much further north than Mammoth Cave. However, the Tortoise Lagoon age model (Petherick et al., 2017) is supported by few dates (Table S1), leaving some uncertainty about the climatic interpretation and timing of those events. A carefully dated, sediment carbon isotope record from Lake Surprise, in southeastern Australia (Falster et al., 2018), shows temporal patterns comparable to the Mammoth Cave record and other Southern Hemisphere records surveyed here. It thus seem likely that the Southern Hemisphere glacial maximum pattern, which clearly extended as far north as Mammoth Cave, at 34°S in Western Australia, also characterized the Late Pleistocene across southern Australia, possibly extending to subtropical latitudes. While the apparently heterogenous expression of southern Australian LGM environments has primarily been accepted at face value (Reeves et al., 2013), the broadly synchronous timing of the onset and termination of full glacial conditions between southwest Western Australia, New Zealand, Patagonia and Antarctica suggests that a unified Southern Hemisphere LGM pattern was conveyed by teleconnections that stretched widely across the hemisphere. If so, we suggest that the most likely explanation for the apparent variability in timing of Australian LGM proxy climate records is simply their variable and often poor age control (Fig. S1). The MC-2 record demonstrates that speleothem palynology, supported by a densely sampled U-Th chronology, can reveal a high resolution history of environmental change that is coherent with other records across much of the Southern Hemisphere.

Acknowledgments

The authors declare no conflict of interest. We thank Mark Delane of the Margaret River Busselton Tourism Association, for facilitating ongoing access to Mammoth Cave; Nick Porch for helpful discussions, Matthias Moros and Patrick DeDeckker for MD03-2611 geochemical data, and Marcus Vandergoes for Galway Tarn pollen data. Data supporting the conclusions of this paper are entirely contained within the paper, references, and Supporting Information. This research was supported by Australian Research Council grant FL160100028 to JDW and FT 130100801 to JH.

Figure legends

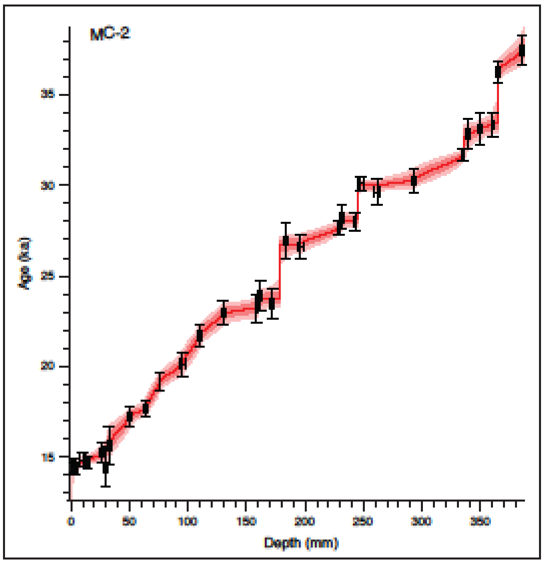
MC-2
Age (ka)
15
20
25
30
35
0
50
100
150
200
250
300
350
Depth (mm)

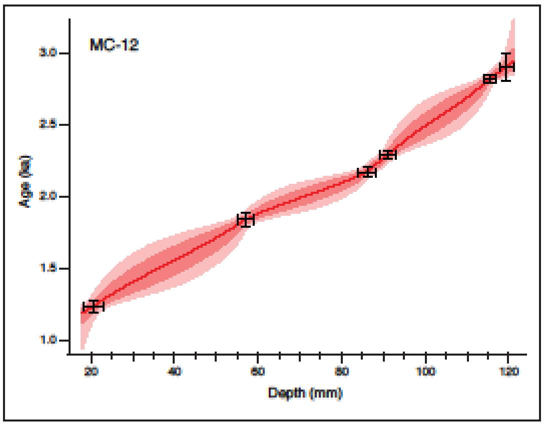
MC-12
Age (ka)
1.0
1.5
2.0
2.5
3.0
20
40
60
80
100
120
Depth (mm)

Figure 1. Age-depth models for stalagmites MC-2 and MC-12, from Mammoth Cave, derived from U-Th ages (Table S2) following (Hendy et al., 2012).

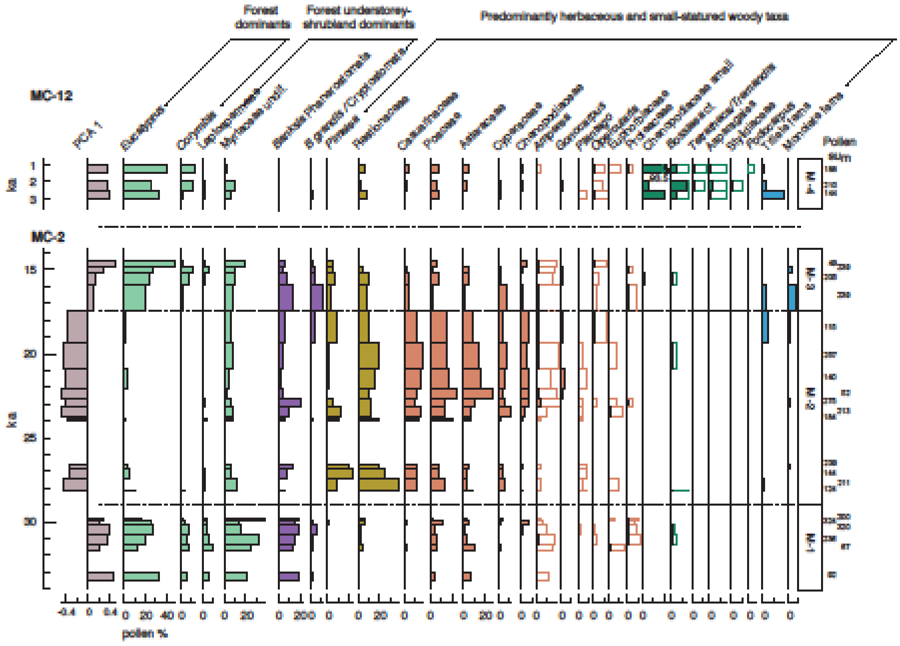
Forest dominants
Forest understorey-shrubland dominants
Predominantly herbaceous and small-statured woody taxa
MC-12
MC-2
PCA 1
Eucalyptus
Corymbia
Leptospermeae
Myrtaceae undiff.
Casuarinaceae
Poaceae
Asteraceae
Cyperaceae
Chenopodiaceae
Brassicaceae
Pollen sum
ka
M-1
M-2
M-3
M-4
15
20
25
30
-0.4
0
0.4
20
40
pollen %

Figure 2. Mammoth Cave pollen percentage record derived from MC-2 and MC-12. *Banksia* is separated into two morphologically distinct groups (Sniderman et al., 2016), small sized grains with affinity to subgenus Phanerostomata, and large grains with affinity to *B. grandis* (Phanerostomata) or subgenus Cryptostomata (Mast and Givnish, 2002).

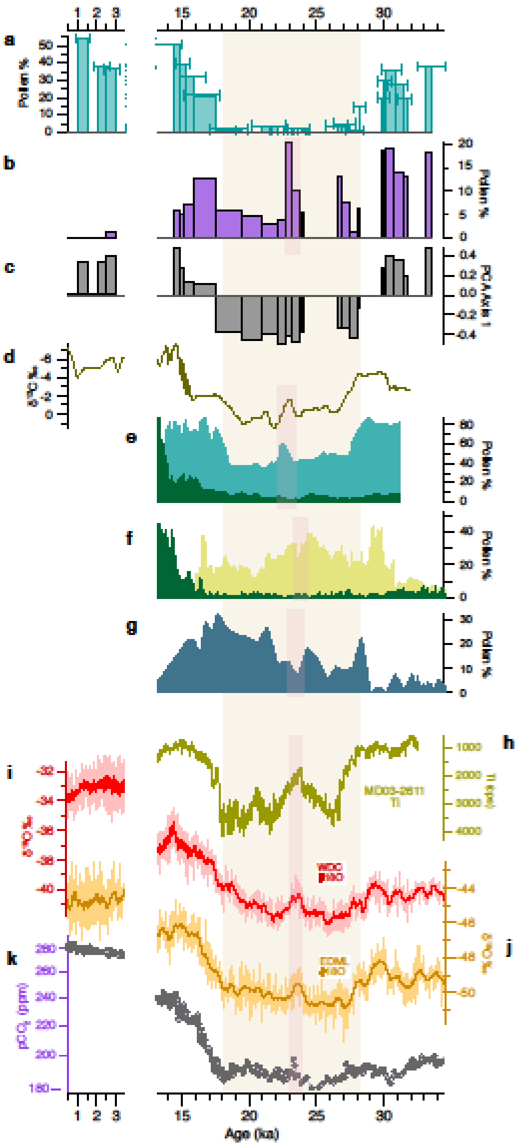
a
b
c
d
e
f
g
h
i
j
k
1
2
3
15
20
25
30
Pollen %
50
40
30
20
10
0
PCA Axis 1
0.4
0.2
0.0
-0.2
-0.4
δ13C ‰
-6
-4
-2
0
80
60
40
MD03-2611
Ti
Ti (cps)
1000
2000
3000
4000
δ18O ‰
-32
-34
-36
-38
-40
WDC
δ18O
EDML
δ18O
-44
-46
-48
-50
pCO2 (ppm)
280
260
240
220
200
180
Age (ka)

Figure 3. Mammoth Cave vegetation compared with other Southern Hemisphere proxy climate records. Pale band demarcates treeless interval at Mammoth Cave, and narrow pink bars demarcates possible correlation of records with AIM 2 event observed in Antarctic ice cores. Mammoth cave (a) eucalypt sum (*Eucalyptus+Corymbia*), (b) *Banksia* sum and (c) first PCA axis. (d) Speleothem δ^{13}C record from Nettlebed, Mt. Arthur, New Zealand, 41.2°S (Hellstrom et al., 1998), plotted according to the modified age model of (Genty et al., 2006). (e) Sum of montane shrubs (turquoise) and Podocarp+angiosperm trees (dark green), excluding *Nothofagus*, from Galway Tarn, at 43.4°S, New Zealand (Vandergoes et al., 2013). (f) Poaceae (yellow) and sum of thermophilous trees (dark green), from Taiquemó, at 42.2°S, southern Chile (Heusser and Heusser, 2006).(g) *Prumnopitys andina* pollen record from Laguna de Tagua Tagua (34.5°S, central Chile(Valero-Garcés et al., 2005). (h) Ti counts per second, a proxy for dust flux, at site MD03-2611, Murray canyon, at 36.7°S, southeastern Australia (De Deckker et al., 2012). Ice core δ^{18}O from (i) West Antarctic Divide Core, 79.5°S (Buizert et al., 2015; Members, 2013; Members et al., 2015) and (j) EDML Core, 75.0°S (Bazin et al., 2013). (k) Composite record of Antarctic ice-core derived atmospheric CO_2 (Bereiter et al., 2015)

References

Alloway, B. V., et al. (2007), Towards a climate event stratigraphy for New Zealand over the past 30 000 years (NZ-INTIMATE project). *Journal of Quaternary Science*, *22*(1), 9-35.

Augustinus, P. A., D. Fink, M.-S. Fletcher, and I. Thomas (2017), Re-assessment of the mid to late Quaternary glacial and environmental history of the Boco Plain, western Tasmania. *Quaternary Science Reviews*, *160*, 31-44.

Barrows, T. T., S. J. Lehman, L. K. Fifield, and P. De Deckker (2007), Absence of cooling in New Zealand and the adjacent ocean during the Younger Dryas Chronozone. *Science*, *318*, 86-89.

Bazin, L., et al. (2013), An optimized multi-proxy, multi-site Antarctic ice and gas orbital chronology (AICC2012): 120–800 ka *Climate of the Past*, *9*, 1715-1731.

Bazin, L., et al. (2013), δ^{18}O measured on ice core EDML on AICC2012 chronology, in *In: Bazin, L et al. (2013): The Antarctic ice core chronology (AICC2012). PANGAEA, https://doi.org/10.1594/PANGAEA.824894*, edited, PANGAEA.

Beard, J. S. (1981), *Vegetation Survey of Western Australia: Swan 1:100 000 Vegetation Series. Explanatory Notes to Sheet 7. The Vegetation of the Swan Area*, University of Western Australia Press, Perth, Western Australia.

Beard, J. S., G. R. Beeston, J. M. Harvey, A. Hopkins, and D. P. Shepherd (2013), The vegetation of Western Australia at the 1:3,000,000 scale. Explanatory Memoir. Second Edition. *Conservation Science Western Australia*, *9*, 1-152.

Bennett, K. D. (2005), *Documentation for psimpoll 4.25 and pscomb 1.03: C programs for plotting pollen diagrams and analysing pollen data*, 127 pp., Uppsala.

Bennett, K. D., and K. J. Willis (2001), Pollen, in *Tracking Environmental Change Using Lake Sediments. Volume 3: Terrestrial, Algal, and Siliceous Indicators.* , edited by J. P. Smol, H. J. B. Birks and W. M. Last, pp. 5-32, Kluwer Academic, Dordrecht.

Bereiter, B., S. Eggleston, J. Schmitt, C. Nehrbass-Ahles, T. F. Stocker, H. Fischer, S. Kipfstuhl, and J. Chappellaz (2015), Revision of the EPICA Dome C CO2 record from 800 to 600 kyr before present. *Geophysical Research Letters*, *42*(2), 542-549.

Black, M. P., S. D. Mooney, and H. A. Martin (2006), A > 43,000-year vegetation and fire history from Lake Baraba, New South Wales, Australia. *Quaternary Science Reviews*, *25*(21-22), 3003-3016.

Bowler, J. M. (1971), Late Quaternary stratigraphy and radiocarbon chronoogy of water level fluctuations in Lake Keilambete, Victoria. *Nature*, *232*, 330-332.

Bowler, J. M., G. S. Hope, J. N. Jennings, G. Singh, and D. Walker (1976), Late Quaternary climates of Australia and New Guinea. *Quaternary Research*, *6*, 359-394.

Brooke, B. P., J. M. Olley, T. Pietsch, P. E. Playford, P. W. Haines, C. V. Murray-Wallace, and C. D. Woodroffe (2014), Chronology of Quaternary coastal aeolianite deposition and the drowned shorelines of southwestern Western Australia – a reappraisal. *Quaternary Science Reviews*, *93*, 106-124.

Builth, H., A. P. Kershaw, C. White, A. Roach, L. Hartney, M. McKenzie, T. Lewis, and G. Jacobsen (2008), Environmental and cultural change on the Mt Eccles lava-flow landscapes of southwest Victoria, Australia. *Holocene*, *18*(3), 413-424.

Buizert, C., et al. (2015), The WAIS Divide deep ice core WD2014 chronology – Part 1: Methane synchronization (68–31 ka BP) and the gas age–ice age difference *Climate of the Past*, *11*, 153-173.

Burke, S. (2004), The feasibility of using charcoal from Devil's Lair, south-west Australia, to access human responses to vegetation changes at the late Pleistocene-Holocene boundary *Australian Archaeology*, *59*, 62-64.

Burney, D. A., and L. P. Burney (1993), Modern pollen deposition in cave sites - experimental results from New-York-State. *New Phytologist*, *124*(3), 523-535.

Chalson, J. M., and H. A. Martin (2008), A 38,000 year history of the vegetation at Penrith Lakes, New South Wales. *Proceedings of the Linnean Society of New South Wales*, *129*, 97-111.

Cheng, H., et al. (2013), Improvements in ^{230}Th dating, ^{230}Th and ^{234}U half-life values, and U–Th isotopic measurements by multi-collector inductively coupled plasma mass spectrometry. *Earth and Planetary Science Letters*, *371–372*, 82-91.

Christensen, P. E. S. (1992), *The Karri Forest: its Conservation, Significance and Manageent*, 188 pp., Department of Conservation and Land Management, Western Australia, Como.

Colhoun, E. A. (1977), A sequence of late Quaternary deposits at Pipe Clay Lagoon, southeastern Tasmania. *Papers and Proceedings of the Royal Society of Tasmania*, *111*, 1-12.

Colhoun, E. A. (1985), Pre-Last Glaciation Maximum vegetation history at Henty Bridge, western Tasmania. *New Phytologist*, *100*, 681-690.

Colhoun, E. A., and A. Goede (1979), The late Quaternary deposits of Blakes Opening and the middle Huon Valley, Tasmania. *Philosophical Transactions of the Royal Society B-Biological Sciences*, *286*, 371-395.

Colhoun, E. A., and G. van de Geer (1986), Holocene to Middle Last Glaciation vegetation history at Tullabardine Dam, western Tasmania. *Proceedings of the Royal Society B-Biological Sciences*, *229*, 177-207.

Colhoun, E. A., and G. van de Geer (1987), Vegetation history and climate before the maximum of the the last glaciation at Crotty, western Tasmania. *Papers and Proceedings of the Royal Society of Tasmania*, *121*, 69-74.

Colhoun, E. A., and G. van der Geer (1988), Darwin Crater, the King and Linda valleys, in *Cainzoic Vegetation of Tasmania*, edited by E. A. Colhoun, pp. 30-71, University of Newcastle, Newcastle, NSW.

Colhoun, E. A., G. van de Geer, and S. J. Fitzsimons (1991), Late glacial and Holocene vegetation history at Governor Bog, King Valley, western Tasmania, Australia. *Journal of Quaternary Science*, *6*, 55-66.

Colhoun, E. A., G. van de Geer, and W. G. Mook (1982), Stratigraphy, pollen analysis, and paleoclimatic interpretation of Pulbeena Swamp, northwestern Tasmania. *Quaternary Research*, *18*, 108-126.

Colhoun, E. A., J. S. Pola, C. E. Barton, and H. Heijnis (1999), Late Pleistocene vegetation and climate history of Lake Selina, western Tasmania. *Quaternary International*, *57/58*, 5-23.

Colhoun, E. A., S. Benger, S. J. Fitzsimons, G. van de Geer, and R. S. Hill (1993), Quaternary organic deposit from Newton Creek Valley, western Tasmania. *Australian Geographical Studies*, *31*, 26-38.

Cook, E. J. (2009), A record of late Quaternary environments at lunette-lakes Bolac and Turangmoroke, Western Victoria, Australia, based on pollen and a range of non-pollen palynomorphs. *Review of Palaeobotany and Palynology*, *153*, 185-224.

Crowley, G. M., and A. P. Kershaw (1994), Late Quaternary Environmental-Change and Human Impact around Lake Bolac, Western Victoria, Australia. *Journal of Quaternary Science*, *9*(4), 367-377.

Cupper, M. L. (2005), Last glacial to Holocene evolution of semi-arid rangelands in southeastern Australia. *The Holocene*, *15*, 541-553.

D'Costa, D. M., P. Edney, A. P. Kershaw, and P. De Deckker (1989), Late Quaternary palaeoecology of Tower Hill, Victoria, Australia. *Journal of Biogeography*, *16*(5), 461-482.

D'Costa, D. M., J. Grindrod, and R. Ogden (1993), Preliminary environmental reconstructions from late Quaternary pollen and mollusc assemblages at Egg Lagoon, King Island, Bass Strait. *Australian Journal of Ecology*, *18*, 351-366.

De Deckker, P., M. Moros, K. Perner, and E. Jansen (2012), Influence of the tropics and southern westerlies on glacial interhemispheric asymmetry. *Nature Geoscience, 5,* 266-269.

De Deckker, P., S. van der Kaars, M. Macphail, and G. Hope (2018), Land-sea correlations in the Australian region: 460 ka of changes recorded in a deep-sea core offshore Tasmania. Part 1: the pollen record. *Australian Journal of Earth Sciences*, *DOI: 10.1080/08120099.2018.1495100*.

Dodson, J. (1977), Late Quaternary palaeoecology of Wyrie Swamp, southeastern South Australia. *Quaternary Research*, *8*, 97-114.

Dodson, J. R. (1975), Vegetation history and water fluctuations at Lake Leake, south-eastern South Australia. II. 50,000 B.P. to 10,000 B.P. *Australian Journal of Botany*, *23*, 815-831.

Dodson, J. R. (1979), Late Pleistocene vegetation and environments near Lake Bullenmerri, western Victoria. *Australian Journal of Ecology*, *4*, 419-427.

Dodson, J. R., and J. J. Lu (2000), A Late Holocene vegetation and environment record from Byenup Lagoon, South-western Australia. *Australian Geographer*, *31*, 41-54.

Dodson, J. R., and R. V. S. Wright (1989), Humid to arid to subhumid vegetation shift on Pilliga Sandstoe, Ulungra Springs, New South Wales. *Quaternary Research*, *32*, 182-192.

Donders, T. H., F. Wagner, and H. Visscher (2006), Late Pleistocene and Holocene subtropical vegetation dynamics recorded in perched lake deposits on Fraser Island, Queensland, Australia. *Palaeogeography Palaeoclimatology Palaeoecology*, *241*(3-4), 417-439.

Dortch, J. (2004), Late Quaternary vegetation change and the extinction of Black-flanked Rock-wallaby (*Petrogale lateralis*) at Tunnel Cave, southwestern Australia. *Palaeogeography Palaeoclimatology Palaeoecology*, *211*, 185-204.

Drysdale, R. N., et al. (2012), Precise microsampling of poorly laminated speleothems for U-series dating. *Quaternary Geochronology*, *14*, 38-47.

Dury, G. H. (1967), Climatic change as a geographical backdrop. *Australian Geographer*, *10*, 231-242.

Ellerton, D., J. Shulmeister, C. Woodward, and P. Moss (2017), Last Glacial Maximum and Last Glacial–Interglacial Transition pollen record from northern NSW, Australia: evidence for a humid late Last Glacial Maximum and dry deglaciation in parts of eastern Australia. *Journal of Quaternary Science*, *32*, 717-728.

Faith, J. T., J. Dortch, C. D. Jones, J. Shulmeister, and K. J. Travouillon (2017), Large mammal species richness and late Quaternary precipitation change in south-western Australia. *Journal of Quaternary Science*, *32*, 760-769.

Falster, G., J. Tyler, K. Grant, J. Tibby, C. Turney, S. Löhr, G. Jacobsen, and A. P. Kershaw (2018), Millennial-scale variability in south-east Australian hydroclimate between 30,000 and 10,000 years ago. *Quaternary Science Reviews*, *192*, 106-122.

Festi, D., D. L. Hoffmann, and M. Luetscher (2016), Pollen from accurately dated speleothems supports alpine glacier low-stands during the early Holocene. *Quaternary Research*, *86*(1), 45-53.

Fitzsimmons, K. E., et al. (2013), Late Quaternary palaeoenvironmental change in the Australian drylands. *Quaternary Science Reviews*, *74*, 78-96.

Fitzsimmons, K. E., N. Stern, C. V. Murray-Wallace, W. Truscott, and C. Pop (2015), The Mungo mega-lake event, semi-arid Australia: non-linear descent into the last ice age, implications for Human behaviour. *Plos One*, *10*(6), e0127008.

Galloway, R. W. (1965), Late Quaternary climates in Australia. *Journal of Geology*, *73*, 603-618.

Genty, D., et al. (2006), Timing and dynamics of the last deglaciation from European and North African $\delta^{13}C$ stalagmite profiles–comparison with Chinese and South Hemisphere stalagmites. *Quaternary Science Reviews*, *25*(17), 2118-2142.

Gouramanis, C., J. Dodson, D. Wilkins, P. De Deckker, and B. M. Chase (2012), Holocene palaeoclimate and sea level fluctuation recorded from the coastal Barker Swamp, Rottnest Island, south-western Western Australia. *Quaternary Science Reviews*, *54*, 40-57.

Harle, K. J. (1997), Late Quaternary vegetation and climate change in southeastern Australia: palynological evidence from marine core E55-6. *Palaeogeography Palaeoclimatology Palaeoecology*, *131*(3-4), 465-483.

Harle, K. J., A. P. Kershaw, and H. Heijnis (1999), The contributions of uranium thorium and marine palynology to the dating of the Lake Wangoom pollen record, western plains of Victoria, Australia. *Quaternary International*, *57-8*, 25-34.

Hellstrom, J. (2003), Rapid and accurate U/Th dating using parallel ion-counting multi-collector ICP-MS. *Journal of Analytical Atomic Spectrometry*, *18*, 1346-1351.

Hellstrom, J. (2006), U–Th dating of speleothems with high initial ^{230}Th using stratigraphical constraint. *Quaternary Geochronology*, *1*(4), 289-295.

Hellstrom, J., M. McCulloch, and J. Stone (1998), A Detailed 31,000-year record of climate and vegetation change, from the isotope geochemistry of two New Zealand speleothems. *Quaternary Research*, *50*, 167-178.

Hendy, E. J., P. J. Tomiak, M. J. Collins, J. Hellstrom, A. W. Tudhope, J. M. Lough, and K. E. H. Penkman (2012), Assessing amino acid racemization variability in coral intra-crystalline protein for geochronological applications. *Geochimica et Cosmochimica Acta*, *86*, 338-353.

Hesse, P. P., J. W. Magee, and S. van der Kaars (2004), Late Quaternary climates of the Australian arid zone: a review. *Quaternary International*, *118-119*, 87-102.

Hesse, P. P., R. Williams, T. J. Ralph, K. A. Fryirs, Z. T. Larkin, K. E. Westaway, and W. Farebrother (2018), Palaeohydrology of lowland rivers in the Murray-Darling Basin, Australia. *Quaternary Science Reviews*, *200*, 85-105.

Heusser, C. J., and L. E. Heusser (2006), Submillennial palynology and palaeoecology of the last glaciation at Taiquemó (50,000 cal yr, MIS 2–4) in southern Chile. *Quaternary Science Reviews*, *25*, 446-454.

Hope, G. (1978), The Late Pleistocene and Holocene vegetational history of Hunter Island, north-western Tasmania. *Australian Journal of Botany*, *6*, 493-514.

Hope, G. (1994), Quaternary vegetation, in *History of the Australian Vegetation: Cretaceous to Recent*, edited by R. S. HIll, pp. 368-389, Cambridge University Press, Cambridge.

Hope, G., J. Coddington, and D. O'Dea (2007), Estuarine development and human occupation at Bobundara Swamp, Tilba Tilba, New South Wales, Australia, in *Wetland Archaeology and Environments: Regional Issues, Global Perspectives*, edited by M. Lillie and S. Ellis, pp. 258-274, Oxbow Books, Oxford.

Hopf, F. V. L., E. A. Colhoun, and C. E. Barton (2000), Late-glacial and Holocene record of vegetation and climate from Cynthia Bay, Lake St Clair, Tasmania. *Journal of Quaternary Science*, *15*(7), 725-732.

Hopper, S. D., and P. Gioia (2004), The southwest Australian floristic region: evolution and conservation of a global hot spot of biodiversity. *Annual Review of Ecology, Evolution, and Systematics*, *35*, 623-650.

Itzstein-Davey, F. (2004), An Early Holocene palaeoenvironmental record from Two Mile Lake, South-Western Australia. *Australian Geographer*, *35*, 317-332.

Kershaw, A. P., D. M. D'Costa, J. R. C. McEwan Mason, and B. E. Wagstaff (1991), Palynological evidence for Quaternary vegetation and environments of mainland southeastern Australia. *Quaternary Science Reviews*, *10*, 391-404.

Kershaw, A. P., D. M. D'Costa, J. R. C. McEwan Mason, and B. E. Wagstaff (1991), Palynological evidence for Quaternary vegetation and environments of mainland southeastern Australia. *Quaternary Science Reviews*, *10*, 391-404.

Kershaw, A. P., G. M. McKenzie, N. Porch, R. G. Roberts, J. Brown, H. Heijnis, M. L. Orr, G. Jacobsen, and P. R. Newall (2007), A high-resolution record of vegetation and climate through the last glacial cycle from Caledonia Fen, southeastern highlands of Australia. *Journal of Quaternary Science*, *22*(5), 481-500.

Ladiges, P. Y., F. Udovicic, and A. N. Drinnan (1995), Eucalypt phylogeny - Molecules and morphology. *Australian Systematic Botany*, *8*(4), 483-497.

Lipar, M., and J. A. Webb (2014), Middle–late Pleistocene and Holocene chronostratigraphy and climate history of the Tamala Limestone, Cooloongup and Safety Bay Sands, Nambung National Park, southwestern Western Australia. *Australian Journal of Earth Sciences*, *61*, 1023-1039.

Longmore, M. E., and H. Heijnis (1999), Aridity in Australia: Pleistocene records of Palaeohydrological and Palaeoecological change from the perched lake sediments of Fraser Island, Queensland, Australia. *Quaternary International*, *57-8*, 35-47.

Mackenzie, L., and P. Moss (2017), A late Quaternary record of vegetation and climate change from Hazards Lagoon, eastern Tasmania. *Quaternary International*, *432*, 58-65.

Martin, A. (1986), Late glacial and Holocene alpine pollen diagrams from the Kosciuscko National Park, New South Wales, Australia. *Review of Palaeobotany and Palynology*, *47*, 367-409.

Martin, H. A. (1973), Palynology and historical ecology of some cave excavations in the Australian Nullarbor. *Australian Journal of Botany*, *21*, 283-316.

Mast, A. R., and T. J. Givnish (2002), Historical biogeography and the origin of stomatal distributions in Banksia and Dryandra (Proteaceae) based on their cpDNA phylogeny. *American Journal of Botany*, *89*(8), 1311-1323.

McGarry, S. F., and C. Caseldine (2004), Speleothem palynology: an undervalued tool in Quaternary studies. *Quaternary Science Reviews*, *23*(23-24), 2389-2404.

McGlone, M. S. (1988), New Zealand, in *Vegetation History*, edited by B. Huntley and T. I. Webb, pp. 557-599, Kluwer, Dordrecht.

McKenzie, G. M. (1997), The late Quaternary vegetation history of the south-central highlands of Victoria, Australia .1. Sites above 900 m. *Australian Journal of Ecology*, *22*(1), 19-36.

Moss, P., J. Tibby, L. Petherick, M. H, and C. Barr (2013), Late Quaternary vegetation history of North Stradbroke Island, Queensland, eastern Australia. *Quaternary Science Reviews*, *74*, 257-272.

Newnham, R. M., D. J. Lowe, T. Giles, and B. V. Alloway (2007), Vegetation and climate of Auckland, New Zealand, since ca. 32 000 cal. yr ago: support for an extended LGM. *Journal of Quaternary Science*, *22*, 517-534.

Newsome, J. C., and E. J. Pickett (1993), Palynology and palaeoclimatic implications of two Holocene sequences from southwestern Australia. *Palaeogeography Palaeoclimatology Palaeoecology*, *101*, 245-261.

Parrenin, F., V. Masson-Delmotte, P. Köhler, D. Raynaud, D. Paillard, J. Schwander, C. Barbante, A. Landais, A. Wegner, and J. Jouzel (2013), Synchronous change of atmospheric CO_2 and Antarctic temperature during the last deglacial warming. *Science*, *339*(6123), 1060-1063.

Pedro, J. B., S. O. Rasmussen, and T. D. van Ommen (2012), Tightened constraints on the time-lag between Antarctic temperature and CO_2 during the last deglaciation. *Climate of the Past*, *8*, 1213-1221.

Petherick, L., et al. (2013), Climatic records over the past 30 ka from temperate Australia – a synthesis from the Oz-INTIMATE workgroup. *Quaternary Science Reviews*, *74*, 58-77.

Petherick, L., P. T. Moss, and H. A. McGowan (2017), An extended Last Glacial Maximum in subtropical Australia. *Quaternary International*, *432*, 1-12.

Pickett, E. J. (1997), The Late Pleistocene and Holocene Vegetation History of Three lacustrine Sequences from the Swan Coastal Plain, Southwestern Australia, PhD thesis, University of Western Australia.

Prentice, I. C., S. F. Cleator, S. P. Harrison, and I. Roultone (2017), Reconstructing ice-age palaeoclimates: Quantifying low-CO_2 effects on plants. *Global and Planetary Change*, *149*, 166-176.

Railsback, L. B., P. L. Gibbard, M. J. Head, N. R. G. Voarintsoa, and S. Toucanne (2015), An optimized scheme of lettered marine isotope substages for the last 1.0 million years, and the climatostratigraphic nature of isotope stages and substages. *Quaternary Science Reviews, 111*, 94-106.

Reeves, J. M., et al. (2013), Climate variability over the last 35,000 years recorded in marine and terrestrial archives in the Australian region: an OZ-INTIMATE compilation. *Quaternary Science Reviews*, *74*, 21-34.

Robbie, A., and H. A. Martin (2007), The History of the Vegetation from the Last Glacial Maximum at Mountain Lagoon, Blue Mountains, New South Wales. *Proceedings of the Linnean Society of New South Wales*, *128*, 57-80.

Scheff, J., R. Seager, H. B. Liu, and S. Coats (2017), Are glacials dry? consequences for paleoclimatology and for greenhouse warming. *Journal of Climate*, *30*, 6593-6609.

Scholz, D., D. L. Hoffmann, J. Hellstrom, and C. Bronk Ramsey (2012), A comparison of different methods for speleothem age modelling. *Quaternary Geochronology*, *14*, 94-104.

Shulmeister, J., G. D. Thackray, T. M. Rittenour, and O. M. Hyatt (2018), Multiple glacial advances in the Rangitata Valley, South Island, New Zealand, imply roles for Southern Hemisphere westerlies and summer insolation in MIS 3 glacial advances. *Quaternary Research*, *89*(2), 375-393.

Sigleo, W. R., and E. A. Colhoun (1981), A short pollen diagram from Crown Lagoon in the Midlands of Tasmania. *Papers and Proceedings of the Royal Society of Tasmania*, *115*, 181-188.

Singh, G., and E. A. Geissler (1985), Late Cainzoic history of vegetation, fire, lake levels and climate, at Lake George, New South Wales, Australia. *Philosophical Transactions of the Royal Society of London B*, *311*, 379-447.

Singh, G., and J. Luly (1991), Changes in vegetation and seasonal climate since the last full glacial at Lake Frome, South Australia. *Palaeogeography Palaeoclimatology Palaeoecology*, *84*, 75-86.

Sniderman, J. M. K., J. D. Woodhead, J. Hellstrom, G. J. Jordan, R. N. Drysdale, J. J. Tyler, and N. Porch (2016), Pliocene reversal of late Neogene aridification. *Proceedings of the National Academy of Sciences*, *113*, 1999-2004.

Stahle, L., C. Whitlock, and S. G. Haberle (2016), A 17,000-Year-Long Record of Vegetation and Fire from Cradle Mountain National Park, Tasmania. *Frontiers in Ecology and Evolution*, *4*, doi: 10.3389/fevo.2016.00082.

Stenni, B., et al. (2010), The deuterium excess records of EPICA Dome C and Dronning Maud Land ice cores (East Antarctica). *Quaternary Science Reviews*, *29*(1), 146-159.

Sturman, A. P., and N. J. Tapper (2006), *The Weather and Climate of Australia and New Zealand*, 541 pp., Oxford University Press, Melbourne.

Sweller, S., and H. A. Martin (2001), A 40,000 year vegetation history and climatic interpretations of Burraga Swamp, Barrington Tops, New South Wales. *Quaternary International*, *83-5*, 233-244.

Turney, C. S. M., et al. (2006), Integration of ice-core, marine and terrestrial records for the Australian Last Glacial Maximum and Termination: a contribution from the OZ INTIMATE group. *Journal of Quaternary Science*, *21*(7), 751-761.

Valero-Garcés, B. L., B. Jenny, M. Rondanelli, A. Delgado-Huertas, S. J. Burns, H. Veit, and A. Moreno (2005), Palaeohydrology of Laguna de Tagua Tagua (34° 30’ S) and moisture fluctuations in Central Chile for the last 46 000 yr. *Journal of Quaternary Science*, *20*(7-8), 625-641.

van de Geer, G., E. A. Colhoun, and W. G. Mook (1986), Stratigraphy, pollen analysis and paleoclimatic interpretation of Mowbray and Broadmeadows Swamps, North Western Tasmania. *Australian Geographer*, *17*, 121-133.

van de Geer, G., L. E. Heusser, J. Lynch-Stieglitz, and C. D. Charles (1994), Paleoenvironments of Tasmania inferred from a 5–75 ka marine pollen recor. *Palynology*, *18*, 33-40.

van de Geer, G., S. J. Fitzsimons, and E. A. Colhoun (1989), Holocene to Middle Last Glaciation vegetation history at Newall Creek, western Tasmania. *New Phytologist*, *111*, 549-558.

van der Kaars, S., G. H. Miller, C. S. M. Turney, E. J. Cook, D. Nürnberg, J. Schönfeld, A. P. Kershaw, and S. J. Lehman (2017), Humans rather than climate the primary cause of Pleistocene megafaunal extinction in Australia. *Nature Communications*, *8*, 14142.

Vandergoes, M. J., R. M. Newnham, G. H. Denton, M. Blaauw, and D. Barrell (2013), The anatomy of Last Glacial Maximum climate variations in south Westland, New Zealand, derived from pollen records. *Quaternary Science Reviews*, *74*, 215-229.

WAIS Divide Project Members., et al. (2015), Precise interpolar phasing of abrupt climate change during the last ice age. *Nature*, *520*, 661.

WAIS Divide Projects Members, et al. (2013), Onset of deglacial warming in West Antarctica driven by local orbital forcing. *Nature*, *500*, 440.

Williams, M., E. Cook, S. van der Kaars, T. Barrows, J. Shulmeister, and P. Kershaw (2009), Glacial and deglacial climatic patterns in Australia and surrounding regions from 35 000 to 10 000 years ago reconstructed from terrestrial and near-shore proxy data. *Quaternary Science Reviews*, *28*, 2398-2419.

Williams, N. J., K. J. Harle, S. J. Gale, and H. Heijnis (2006), The vegetation history of the last glacial-interglacial cycle in eastern New South Wales, Australia. *Journal of Quaternary Science*, *21*(7), 735-750.

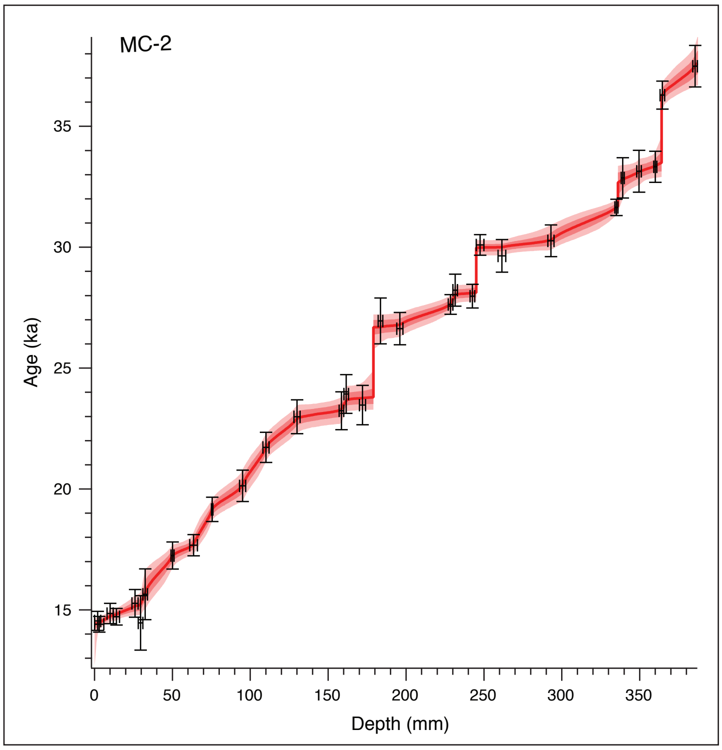
MC-2
Age (ka)
15
20
25
30
35
Depth (mm)
0
50
100
150
200
250
300
350

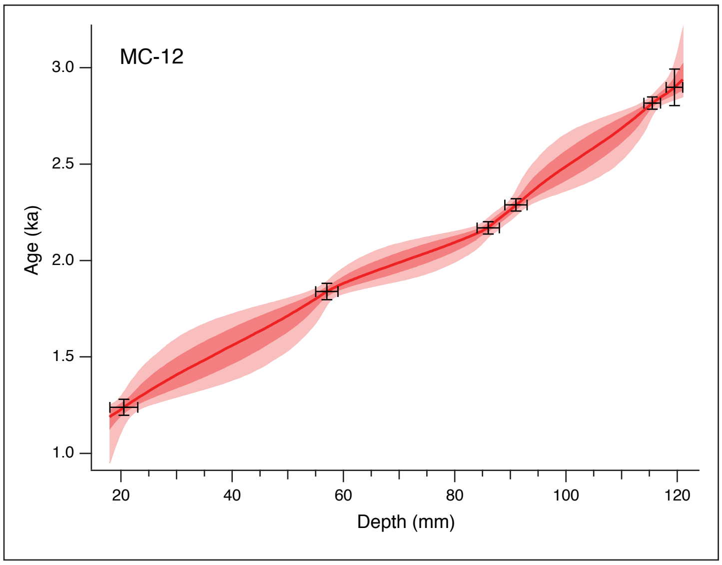
MC-12
Age (ka)
1.0
1.5
2.0
2.5
3.0
Depth (mm)
20
40
60
80
100
120


Forest dominants
Forest understorey-shrubland dominants
Predominantly herbaceous and small-statured woody taxa
MC-12
MC-2
PCA 1
Eucalyptus
Corymbia
Leptospermeae
Myrtaceae undif.
Banksia Phanerostomata
B grandis / Cryptostomata
Pimelea
Restionaceae
Casuarinaceae
Poaceae
Asteraceae
Cyperaceae
Chenopodiaceae
Amperea
Gonocarpus
Plantago
Opercularia
Euphorbiaceae
Proteaceae
Chenopodiaceae small
Bossiaea cf.
Tetratheca/Tremandra
Asparagales
Stylidiaceae
Podocarpus
Trilete ferns
Monolete ferns
Pollen sum
ka
1
2
3
15
20
25
30
93.5
188
210
144
49
239
205
239
115
257
140
52
275
213
184
239
144
211
124
324
200
320
236
67
92
M-4
M-3
M-2
M-1
-0.4
0
0.4
0
20
40
0
0
0
20
0
20
0
0
0
20
0
0
0
20
0
0
0
0
0
0
0
0
0
0
0
0
0
0
0
pollen %

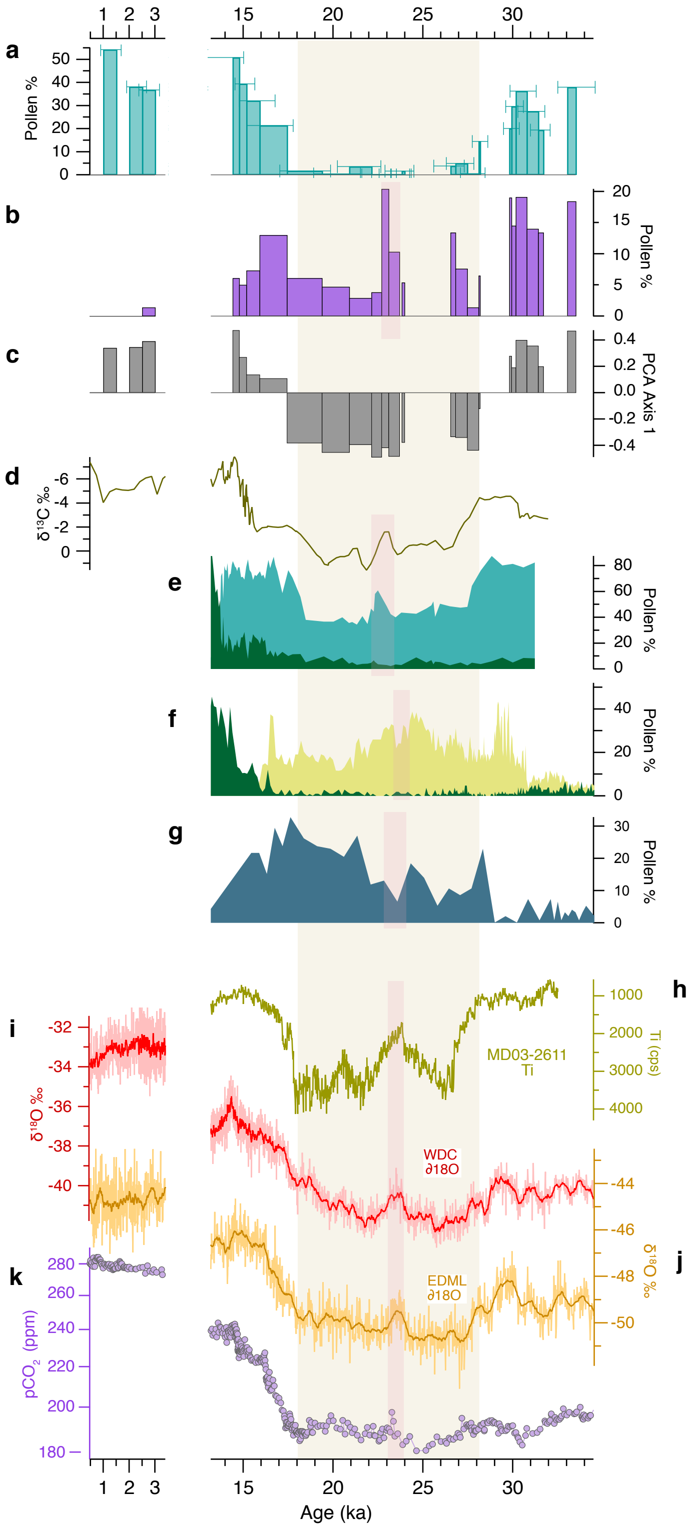
a
b
c
d
e
f
g
h
i
j
k
Pollen %
PCA Axis 1
δ13C ‰
MD03-2611 Ti
Ti (cps)
WDC ∂18O
EDML ∂18O
δ18O ‰
pCO2 (ppm)
Age (ka)
1
2
3
15
20
25
30